JACS
JOURNAL OF THE AMERICAN CHEMICAL SOCIETY
Article
pubs.acs.org/JACS

Cyclobutane Thymine Photodimerization Mechanism Revealed by Nonadiabatic Molecular Dynamics

Clemens Rauer, Juan J. Nogueira, Philipp Marquetand,* and Leticia González*

Institute of Theoretical Chemistry, Faculty of Chemistry, University of Vienna, Währinger Straße 17, 1090 Vienna, Austria

Supporting Information

ABSTRACT: The formation of cyclobutane thymine dimers is one of the most important DNA carcinogenic photolesions induced by ultraviolet irradiation. The long debated question whether thymine dimerization after direct light excitation involves singlet or triplet states is investigated here for the first time using nonadiabatic molecular dynamics simulations. We find that the precursor of this [2 + 2] cycloaddition reaction is the singlet doubly $\pi^2\pi^{*2}$ excited state, which is spectroscopically rather dark. Excitation to the bright $^1\pi\pi^*$ or dark $^1n\pi^*$ excited states does not lead to thymine dimer formation. In all cases, intersystem crossing to the triplet states is not observed during the simulated time, indicating that ultrafast dimerization occurs in the singlet manifold. The dynamics simulations also show that dimerization takes place only when conformational control happens in the doubly excited state.

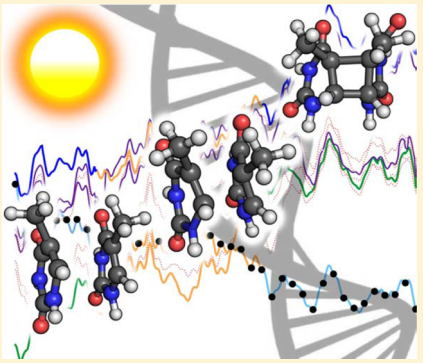

1. INTRODUCTION

Exposure to ultraviolet (UV) radiation can damage DNA.[1] The deleterious action of UV light originates from the photochemical changes that lead to biological alterations. One harmful reaction occurring in DNA after light absorption that eventually causes skin cancer is the formation of intrastrand cyclobutane thymine dimers.[2] Although the existence of T <> T dimers was already reported in the 1960s,[3−5] the molecular details of this photoreaction still remain controversial. During the past decade, intensive experimental[6−10] and theoretical[11−18] research has debated the involvement of singlet or triplet electronic excited states in the formation of T <> T dimers. According to femtosecond (fs) time-resolved infrared experiments on thymine single strands, cyclobutane thymine dimers are fully formed in less than 1 ps as a result of a barrierless decay of the electronic singlet $^1\pi\pi^*$ state.[9,10] This view has been challenged by another fs time-resolved experiment,[6] which identified a triplet state as a major precursor of cyclobutane thymine dimer formation. Later time-resolved and steady-state experiments found the contribution of the $^3\pi\pi^*$ state to be smaller than 10%,[11] in agreement with the identification by nanosecond (ns) spectroscopy of a long-lived nonreactive triplet intermediate.[8]

Quantum chemical calculations have also attributed the ultrafast nature of this reaction to internal conversion from the lowest singlet $^1\pi\pi^*$ excited state to the ground state.[12,13,15,17] Interestingly, ref 12 characterizes this state as a doubly excited state, while others, e.g. refs 15, 17, report the state to be singly excited. Reaction pathways claiming the participation of the $^3\pi\pi^*$ state have also been calculated.[18,19] In addition to direct excitation, T <> T dimers can also form under triplet photosensitization. In the latter case, it is well established that the reaction proceeds via triplet states: After excitation, a photosensitizer undergoes intersystem crossing and then transfers its energy to a thymine molecule, thereby promoting the latter to its triplet state. This triplet thymine then reacts with another thymine in the ground state and gives the final adduct.[19−22] Despite the dimer yield being low for both sensitized and direct UV excitation cases,[21] the mechanism for the reaction in the absence or presence of a photosensitizer might be very different.

In this paper we investigate whether UV exposure triggers T <> T dimer formation in the singlet or triplet manifold. To this aim, we report the first ab initio nonadiabatic molecular dynamics simulations of a stacked thymine dimer including all relevant singlet and triplet states. The calculations are performed in gas phase using the surface-hopping including arbitrary couplings (SHARC) scheme[23,24] coupled to multiconfigurational state-average complete active space self-consistent field[25] (SA-CASSCF) energies, gradients, and spin−orbit couplings (see computational details in Section S1 of the Supporting Information (SI)).

2. RESULTS AND DISCUSSION

2.1. Dynamics Simulations. Formally, the formation of T <> T dimers is a [2 + 2] cycloaddition in which two adjacent stacked thymines are linked via the C_5−C_6 bonds forming a cyclobutane ring (see Figure 1). Insight about this and other concerted pericyclic reactions can be gained by means of the Woodward−Hoffmann rules.[26] These rules forbid a thermal dimerization in the ground state; however, they do not prescribe whether photochemical dimerization should proceed in the singly excited (^{1}SE) or doubly excited (^{1}DE) state. For

Received: June 29, 2016
Published: September 28, 2016

DOI: 10.1021/jacs.6b06701
J. Am. Chem. Soc. 2016, 138, 15911−15916

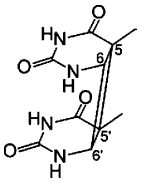

Figure 1. Cyclobutane thymine dimer with labeling of the forming bonds.

the sake of later discussion of the states involved in the dimerization of thymine, the orbital and singlet state correlation diagrams of the [2 + 2] cycloaddition of ethylene are shown in Figure 2. In agreement to the Woodward–Hoffmann rules,

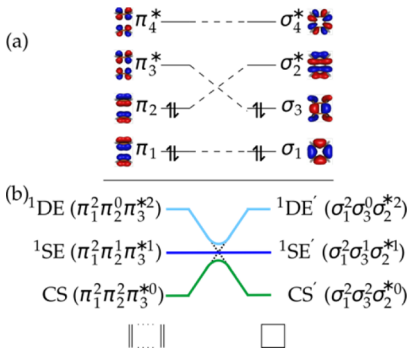

Figure 2. Woodward–Hoffmann orbital (a) and state (b) correlation diagrams for the [2 + 2] cycloaddition of two ethylene molecules on singlet surfaces. DE (doubly excited), SE (singly excited), and CS (closed-shell) states are indicated by cyan, blue, and green, respectively.

ethylene dimerization is thermally forbidden, as the ground state changes its character from one closed shell (CS) configuration, with orbital occupation $\pi_1^2\pi_2^2$, to another closed shell configuration, CS′($\sigma_1^2\sigma_3^2$). Photochemically, the reaction is allowed from the ^{1}SE or ^{1}DE state. During the course of the reaction, the involved states can be classified in two ways: (1) according to the orbital evolution and (2) according to the number of excited electrons. Looking at the first criterion, the ^{1}DE state evolves into the CS′ state (dashed curve in Figure 2b, called diabatic representation in the following). Analogously, the initial ground state CS evolves into the ^{1}DE′ state and ^{1}SE into ^{1}SE′. According to the second criterion, the number of excited electrons, the ^{1}DE corresponds to the ^{1}DE′ (solid curves in Figure 2b, called adiabatic representation in the following) and similarly CS to CS′ as well as ^{1}SE to ^{1}SE′. Dimerization of ethylene occurs from the singlet ^{1}DE state potential.[27−29] Interestingly, a direct comparison of the role of ^{1}SE and ^{1}DE states in the cyclobutane thymine dimer formation is absent in the literature, mostly because the majority of papers dealing with this reaction employ theoretical methods, such as density functional theory, unable to describe DE states.[11,18,30−32] Here, in contrast, we employ multiconfigurational methods which can describe DE states.

To answer the question about the precursor state, trajectories in full dimensionality were run starting from all eligible states: the ^{1}DE($\pi\pi^*$), ^{1}SE($\pi\pi^*$), and ^{1}nπ^* states. For each of these trajectories, the respective gradients and couplings determine which state will be subsequently populated; then, at every geometry, the energies of the other states are calculated vertically. The starting geometries of the trajectories are taken from the static calculations reported in ref 13. In these geometries, the initial separation of the C_5-C_5' and C_6-C_6' bonds is slightly above 3 Å, mimicking the shortest distances found in previous ground-state molecular dynamics simulations of DNA.[33]

We first discuss the dynamics started in the ^{1}DE state, for which 5 out of the 10 trajectories showed dimerization. We note that the purpose of these dynamics simulations is to find possible dimerization pathways and not to provide statistical information regarding reaction rates or time constants. In Figure 3, the evolution in time of the relevant energy levels

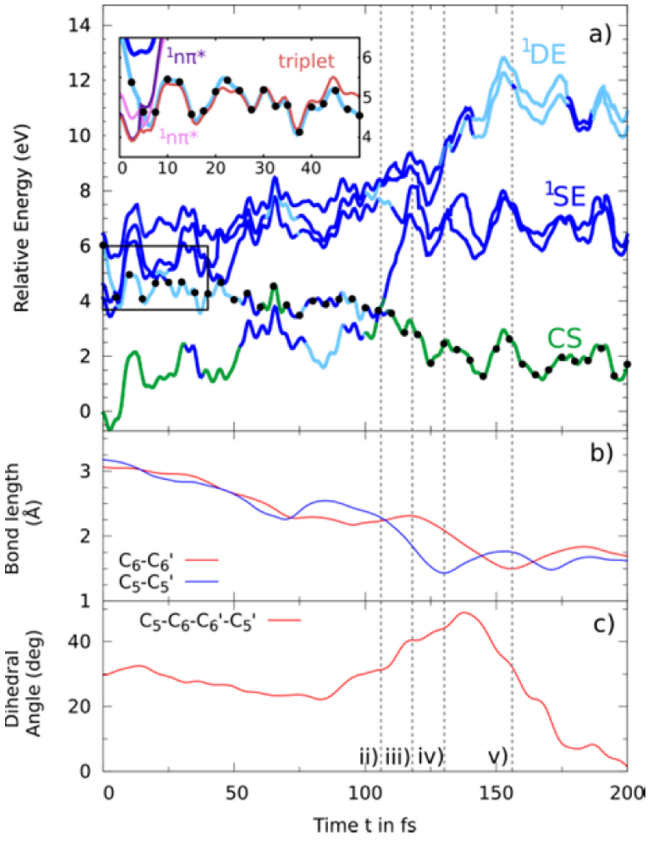

Figure 3. Time evolution of energy levels (a), the C_5-C_5' and C_6-C_6' distances (b), and the dihedral angle $\eta(C_5-C_6-C_6'-C_5')$ between them (c) for a reactive trajectory started from the doubly excited state (^{1}DE). The black dots indicate which state is populated. The color code in panel (a) is similar to that in Figure 2: green for closed-shell (CS), blue for singly excited (SE) states (both nπ^* and $\pi\pi^*$), cyan for doubly excited (DE) states. The first 50 fs are zoomed in the inset. Diabatic states, including nπ^* states (pink and violet), $\pi\pi^*$ states (blue (SE) and cyan (DE)), and triplet states (red), are displayed. Vertical lines in panels (a–c) indicate the times corresponding to the geometries displayed in Figure 4.

(panel a), the C_5-C_5' and C_6-C_6' distances (b), and the dihedral angle $\eta(C_5-C_6-C_6'-C_5')$ (c) are shown for one example reactive trajectory (see also Figure S4). Following the diabatic states along the reaction is only possible at the beginning of the trajectory (inset of Figure 3a), when the separation between the two nucleobases is still large and the identification of the orbitals is clear. Once the C–C bonds start to form, the four frontier π orbitals evolve toward four σ orbitals (recall Figure 2) and other remaining orbitals become energetically degenerated, undergoing strong mixing. As a consequence, diabatic characterization of the electronic states is

DOI: 10.1021/jacs.6b06701
J. Am. Chem. Soc. 2016, 138, 15911−15916

hardly possible and Figure 3a shows the adiabatic evolution of the states. In this representation, the electronic states can have closed-shell, singly excited, or doubly excited character (see more details in Section S1.3 of the SI).

The underlying mechanism for the reactive trajectory elegantly complies with the simple Woodward–Hoffmann correlation diagrams discussed for the [2 + 2] cycloaddition of ethylene: The system initially evolves on the ^{1}DE state during the first 50 fs. Then, the character of the populated electronic state becomes adiabatically singly excited. After ca. 120 fs, the populated state is of closed-shell character, which corresponds to the CS′ (ground state) in Figure 2. The inset of Figure 3a shows the further complexity involved in the deactivation: At the considered initial geometry (Figure 4i), the ^{1}DE state

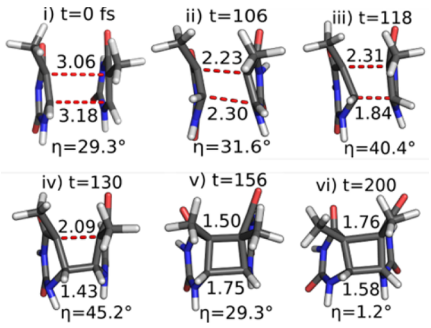

Figure 4. Geometrical snapshots of the reactive trajectory depicted in Figure 3. C_5–C_5' and C_6–C_6' distances in angstroms and dihedral angles $\eta(C_5$–C_6–C_6'–$C_5')$ in degrees.

corresponds to the S_3 state, which crosses after a few femtoseconds with two electronic states (mainly of ^{1}nπ^* character) and thereby becomes adiabatically the S1 state within less than 50 fs. The hopping geometries for the S3/S2 and S_2/S_1 crossing points are very similar to the initial geometry because this geometry is already quite close to the crossing area. The deactivation to the ground state proceeds via the S_1/S_0 conical intersection (Figure 4ii), which is different from the crossing point reported by Blancafort et al.[12] (probably due to a differing reactant geometry) but identical to the crossing point proposed by Boggio-Pasqua et al.[13] At this geometry, both C_5–C_5' and C_6–C_6' distances are very similar, but the C_5–C_5' bond is shorter indicating the preference for the first bond to be formed. Indeed, the C_5–C_5' bond is formed earliest in all the reactive trajectories. The cyclobutane ring is then only fully created in the electronic ground state. The evolution of the C_5–C_5' and C_6–C_6' distances (Figure 3b) shows that the C_5–C_5' bond is established first (Figures 4iii and 4iv) and, after ca. 30 fs, the C_6–C_6' bond formation follows (Figure 4v), illustrating the "concertedness" of this pericyclic reaction, in the spirit of the Woodward–Hoffmann rules. The snapshot at 200 fs (Figure 4vi) shows how the newly formed bonds asynchronously alternate in time, due to excess vibrational energy.

Dimerizable conformers at the chosen initial geometry have a dihedral angle close to that of B-DNA (η = 33°).[34] During the reaction, η decreases concomitantly with the C_5–C_5' and C_6–C_6' distances (Figure 3b–c). This is the case for all reactive trajectories (see Figure S2), which hints at conformational control, as suggested e.g. in refs 29, 33. Around the S_1/S_0 conical intersection, when the two stacked thymines are separated by ca. 2.3 Å, the dihedral angle starts increasing to avoid sterical clashes. After deactivation to the ground state, the dihedral angle continues increasing to 45°, until the C_5–C_5' bond is formed (Figure 4iv). As the cyclobutane ring develops the two thymines get perfectly aligned in space (see Figure 3c and Figure 4vi).

In the nonreactive trajectories starting from the ^{1}DE state, the system quickly relaxes to the ^{1}nπ^* states and stays in the lowest one, which is then the S1 state (see one example in Figure 5a and Figure S5). The characterization of electronic

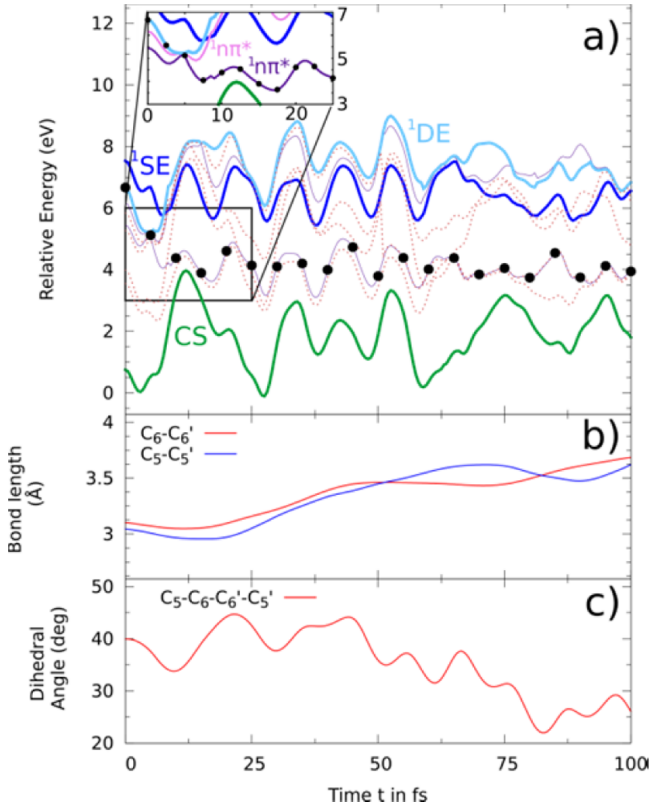

Figure 5. Time evolution of energy levels (a), the C_5–C_5' and C_6–C_6' distances (b) and the dihedral angle $\eta(C_5$–C_6-C_6'-$C_5')$ between them (c) for a nonreactive trajectory started from the double excited state (^{1}DE). The black dots indicate which state is populated. The color code is the same as that in the inset of Figure 3a.

states for nonreactive trajectories is easier than for the reactive ones since due to the large separation between the two thymines, there is no orbital mixing. Accordingly, the states of Figure 5a can be plotted in the diabatic representation, where the character of the wavefunction is maintained. In most trajectories, during the first 50 fs the thymines move apart and η increases (Figure S3), preventing dimerization and suggesting that indeed conformational control steers the reaction. However, the nonreactive trajectory of Figure 5 serves as a counterexample. The general trend of η is a continuous decrease (Figure 5c), which nonetheless does not lead to dimerization (Figure 5b) because the system is in the ^{1}nπ^* state. This behavior demonstrates not only that conformational control is not the only factor determining T <> T dimerization but also that electronic effects play a key role. Our simulations predict that only when the trajectories occupy the state with double excitation character and the dihedral angle decreases, dimerization takes place.

DOI: 10.1021/jacs.6b06701
J. Am. Chem. Soc. 2016, 138, 15911–15916

All the trajectories initiated in the bright ^{1}SE state (S_4) are not reactive, at least during the first 200 fs in which we propagated. In all cases (see one example in Figure S6), the system stays in the S4 for the complete propagation time without undergoing internal conversion to lower states, while C_5-C_5' and C_6-C_6' distances increase. Although we did not expect dimerization in the $^1n\pi^*$ states, trajectories were also run from the lowest $^1n\pi^*$ state, which is the S_1 state (Figure S7), but indeed T <> T is not formed and the system also does not relax to the ground state in the time simulated.

A key question is whether triplet electronic states are involved in the dimerization. In principle, it is conceivable that a triplet state is populated by singlet fission,[35] where a monomer in a singlet excited state transfers part of its electronic energy to a neighboring ground state monomer, resulting in the population of low lying triplet states of both monomers. As a result, the whole system has double-excitation character and singlet spin multiplicity. This process is energetically favorable only if the triplet excitation energy of the monomer is half of the singlet electronic state energy of the dimer. According to literature calculations[36] performed at the complete active space second-order perturbation (CASPT2) level of theory, the energies of the bright singlet state of the thymine−thymine reactant and the lowest triplet state of a single thymine at the Franck−Condon geometry are 4.89 and 3.59 eV, respectively. Since the energy requirements are not fulfilled, singlet fission is not possible in this region. However, the energies of the electronic excited states can strongly change along the dynamics, and the energetic requirement for singlet fission could be met at certain geometries. However, the energetic criterion is not the only requirement for singlet fission, but also a particular electronic configuration is needed. To investigate the latter, we have analyzed the character of the ^{1}DE state in the reactive trajectories. By looking at the wave function, it is possible to identify whether after excitation the electrons are located in both monomers (Figure 6a−b) or in one (Figure 6c). Only the electronic configuration of Figure 6a complies with the definition of singlet fission. Unfortunately, configurations 6a and 6b cannot be distinguished in our analysis. Therefore, it will be assumed that both of them are products of singlet fission, overestimating the contribution of this process. During the time the ^{1}DE state is populated (from 0 to 50 fs), we obtain a maximum of 35% of singlet fission probability. This means that the probability of the double excitation being located in one monomer is, at least, 65% and thus singlet fission only plays a minor role.

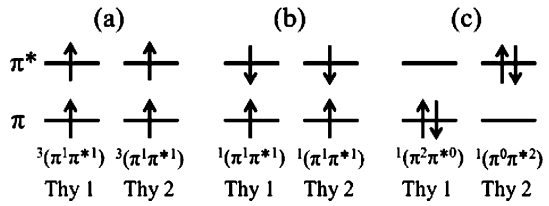

Figure 6. Electronic configurations of the thymine monomers that can compose the singlet doubly excited state ^{1}DE in the dimer.

The second way to populate a triplet state is via intersystem crossing, as proposed by Kwok et al.[6] The present simulations show that even when the potentials of the populated singlet state and a triplet state lie close in energy for a long period of the trajectory, the system does not undergo intersystem crossing due to the very small spin−orbit coupling. For instance (see inset of Figure 3a), at 15 fs, the ^{1}DE and the triplet T_3 state are separated by 0.032 eV (258 cm^{-1}) and the corresponding spin−orbit coupling is 0.03 cm^{-1}. Note that a CASPT2 calculation gives values of 0.33 eV (2662 cm^{-1}) and 0.19 cm^{-1}, respectively, so that the ratio between energy gap and coupling is of the same order of magnitude in both cases, and it does not change the conclusion that ISC does not occur. The absence of intersystem crossing is observed in all the trajectories (see SI), regardless of being reactive or nonreactive. We therefore conclude that the triplet states do not play a role in the ultrafast dimerization pathway induced by UV excitation, in agreement with Kohler and co-workers.[10]

2.2. Effect of the Environment. Our nonadiabatic molecular dynamics simulations have been performed in the gas phase. However, the cyclobutane thymine dimerization takes place in biological systems and the experimental measurements are generally performed for solvated single strands.[6−11] To investigate the effect of the biological environment, we have selected three snapshots from the reactive trajectory shown in Figure 3 at simulation times 10, 100, and 190 fs, i.e. in the reactant, S_1/S_0 conical intersection, and product regions, respectively. The three dimer structures were embedded in a solvated single strand $(dT)_{12}$, and the excitation energies were calculated by an electrostatic quantum mechanics/molecular mechanics (QM/MM) scheme.[37] The reactive thymine dimer was treated at the SA-CASSCF level,[25] and the environment was described by the Amber force field.[38] Further details can be found in Section S1.4 of the SI.

The QM/MM excitation energies (Table S1) show that the environment has a minor effect in the regions of reactants and S_1/S_0 conical intersection. The electrostatic interactions with the strand and solvent induce a small shift of ca. 0.1 eV in the $^{1,3}\pi\pi^*$ states, which according to the dynamics simulations are the relevant states. The effect of the environment is more important for the products, changing the order of some highly excited states. However, this is irrelevant because when the reaction is close to the product region, the system is already in the electronic ground state, which is well separated from the excited states. The negligible effect of the electrostatic interactions on the dimerization process agrees with previous density functional theory calculations[11] performed in gas-phase and water solution using a polarizable continuum model. However, this does not mean that the environment has a passive role. For example, QM/MM calculations including four nucleobases in the QM region predicted that thymine dimerization can be quenched by electron transfer from a flanking guanine nucleobase.[15,17]

Our QM/MM calculations also demonstrate that the triplet states do not participate in the dimerization process, corroborating the gas phase dynamical simulations. The singlet/triplet energy gaps and spin−orbit couplings in the presence of the biological environment are very similar to the gas phase values. For example, at 10 fs, the energy gap and spin−orbit coupling between the relevant ^{1}DE state and the closest triplet state T_3 are 0.12 eV (968 cm^{-1}) and 0.54 cm^{-1}, in the solvated strand versus 0.10 eV (807 cm^{-1}) and 0.59 cm^{-1}, respectively, in the gas phase. Note that the spin−orbit coupling between the same states within the Franck−Condon region, as calculated from 20 different conformations from the QM/MM dynamics, is only of the order of 10^{-2} cm^{-1} for all the geometries.

DOI: 10.1021/jacs.6b06701
J. Am. Chem. Soc. 2016, 138, 15911−15916

2.3. Populating the Doubly Excited State. We have shown that thymine dimerization requires the population of a singlet doubly excited state ^{1}DE. However, due to its double excitation character, this state lies high in energy, and the pathway to populate it is still an open question. Two possibilities can be conceived: (i) direct excitation under UV radiation or (ii) nonradiative relaxation from the bright singly excited state ^{1}SE. In order to investigate the first route, we have calculated the absorption spectrum of the thymine dimer embedded in a solvated single strand $(dT)_{12}$ using a QM/MM scheme and 250 geometries sampled from ground state molecular dynamics. The two nucleobases in the middle of the strand were described by the multistate CASPT2 (MS-CASPT2) method[39] and the rest of the system by the Amber force field.[38] All the states were characterized as singly or doubly excited states by analyzing their one-electron transition density matrix.[40,41] More details can be found in Section S1.5 of the SI. The resulting absorption spectrum decomposed into ^{1}SE and ^{1}DE states is shown in Figure 7. The ^{1}DE state lies at

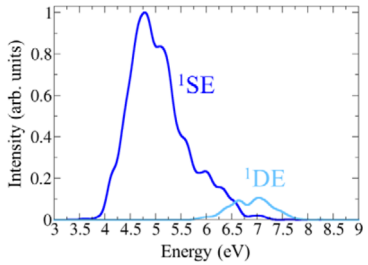

Figure 7. Absorption spectrum of the ^{1}SE and ^{1}DE states of the thymine dimer embedded in a $(dT)_{12}$ single strand calculated at MS-CASPT2/Amber level of theory.

energies larger than 6 eV, which is well above the usual experimental excitation energy[6,9,10] of 4.5 eV. We conclude, therefore, that the population of the ^{1}DE state by direct excitation is not possible. Accordingly, the ^{1}DE state should be populated nonradiatively from the bright ^{1}SE state through a ^{1}SE/^{1}DE conical intersection or through crossings with other electronic states. Since the ^{1}SE and ^{1}DE states are almost degenerate at the beginning of the dynamics (see inset of Figure 3a), we believe that there should be a conical intersection close to the Franck–Condon region although we were not able to locate it because of the large configurational space involved. Moreover, since the yield of the reaction is less than 5%,[9−11] this conical intersection should be slightly above the energy of the bright ^{1}SE state, as sketched in Figure 8. Note that this mechanism is different from the proposed barrierless

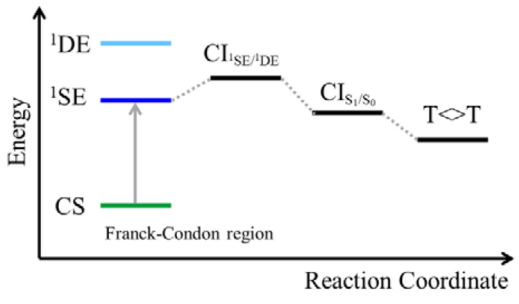

Figure 8. Suggested mechanism to populate the ^{1}DE state from ^{1}SE, and subsequent evolution of the dimerization.

pathways from refs 11−13, 15−17, where the low yield of the reaction is then attributed to conformational control in the ground state originally suggested in refs 29, 33. After populating the ^{1}DE state, our dynamics simulations have shown that the system evolves along the reaction coordinate toward the S_1/S_0 conical intersection, from where the cyclobutane dimer is formed.

3. CONCLUSIONS

In conclusion, our ab initio molecular dynamics simulations show that ultrafast cyclobutane thymine dimerization requires populating the singlet doubly excited state, ^{1}DE. The reaction occurs without the participation of triplet states, neither by intersystem crossing nor by singlet fission. We also show that, besides conformational control, electronic effects are essential to promote cyclobutane formation. The doubly excited state cannot be populated by direct excitation because it lies at a higher energy than the commonly employed laser wavelengths or the UV spectrum of the sun at the earth's surface. We propose that the population of the reactive state should happen by internal conversion from the bright singly excited state, possibly by overcoming a small energy barrier, thus explaining the low yield of the reaction. However, further calculations are necessary to clarify this point.

■ ASSOCIATED CONTENT

Supporting Information

The Supporting Information is available free of charge on the ACS Publications website at DOI: 10.1021/jacs.6b06701.

Further information on computational details, the time evolution of energies and important coordinates, and the S_1/S_0 conical intersection geometry are given (PDF)

■ AUTHOR INFORMATION

Corresponding Authors

*philipp.marquetand@univie.ac.at

*leticia.gonzalez@univie.ac.at

Notes

The authors declare no competing financial interest.

■ ACKNOWLEDGMENTS

C.R. gratefully acknowledges the University of Vienna within the uni:docs programme for financial support. The computational results have been achieved in part using the Vienna Scientific Cluster (VSC). The authors thank M. Boggio-Pasqua for fruitful discussions.

■ REFERENCES

(1) Friedberg, E. C. *Nature* **2003**, *421*, 436−440.
(2) Mouret, S.; Baudouin, C.; Charveron, M.; Favier, A.; Cadet, J.; Douki, T. *Proc. Natl. Acad. Sci. U. S. A.* **2006**, *103*, 13765−13770.
(3) Beukers, R.; Berends, W. *Biochim. Biophys. Acta* **1960**, *41*, 550−551.
(4) Setlow, R. B.; Setlow, J. K. *Proc. Natl. Acad. Sci. U. S. A.* **1962**, *48*, 1250−1257.
(5) Setlow, R. B.; Swenson, P. A.; Carrier, W. L. *Science* **1963**, *142*, 1464−1466.
(6) Kwok, W. M.; Ma, C.; Phillips, D. L. *J. Am. Chem. Soc.* **2008**, *130*, 5131−5139.
(7) Marguet, S.; Markovitsi, D. *J. Am. Chem. Soc.* **2005**, *127*, 5780−5781.
(8) Pilles, B. M.; Bucher, D. B.; Liu, L.; Clivio, P.; Gilch, P.; Zinth, W.; Schreier, W. J. *J. Phys. Chem. Lett.* **2014**, *5*, 1616−1622.

DOI: 10.1021/jacs.6b06701
J. Am. Chem. Soc. 2016, 138, 15911−15916

(9) Schreier, W. J.; Kubon, J.; Regner, N.; Haiser, K.; Schrader, T. E.; Zinth, W.; Clivio, P.; Gilch, P. *J. Am. Chem. Soc.* **2009**, *131*, 5038−5039.
(10) Schreier, W. J.; Schrader, T. E.; Koller, F. O.; Gilch, P.; Crespo-Hernández, C. E.; Swaminathan, V. N.; Carell, T.; Zinth, W.; Kohler, B. *Science* **2007**, *315*, 625−629.
(11) Banyasz, A.; Douki, T.; Improta, R.; Gustavsson, T.; Onidas, D.; Vayá, I.; Perron, M.; Markovitsi, D. *J. Am. Chem. Soc.* **2012**, *134*, 14834−14845.
(12) Blancafort, L.; Migani, A. *J. Am. Chem. Soc.* **2007**, *129*, 14540−14541.
(13) Boggio-Pasqua, M.; Groenhof, G.; Schäfer, L. V.; Grubmüller, H.; Robb, M. A. *J. Am. Chem. Soc.* **2007**, *129*, 10996−10997.
(14) González-Ramírez, I.; Roca-Sanjuán, D.; Climent, T.; Serrano-Pérez, J. J.; Merchán, M.; Serrano-Andrés, L. *Theor. Chem. Acc.* **2011**, *128*, 705−711.
(15) Lee, W.; Matsika, S. *Phys. Chem. Chem. Phys.* **2015**, *17*, 9927−9935.
(16) Serrano-Pérez, J. J.; González-Ramírez, I.; Coto, P. B.; Merchán, M.; Serrano-Andrés, L. *J. Phys. Chem. B* **2008**, *112*, 14096−14098.
(17) Spata, V. A.; Lee, W.; Matsika, S. *J. Phys. Chem. Lett.* **2016**, *7*, 976−984.
(18) Zhang, R. B.; Eriksson, L. A. *J. Phys. Chem. B* **2006**, *110*, 7556−7562.
(19) Climent, T.; González-Ramírez, I.; González-Luque, R.; Merchán, M.; Serrano-Andrés, L. *J. Phys. Chem. Lett.* **2010**, *1*, 2072−2076.
(20) Cuquerella, M. C.; Lhiaubet-Vallet, V.; Bosca, F.; Miranda, M. A. *Chem. Sci.* **2011**, *2*, 1219−1232.
(21) Liu, L.; Pilles, B. M.; Gontcharov, J.; Bucher, D. B.; Zinth, W. *J. Phys. Chem. B* **2016**, *120*, 292−298.
(22) Miro, P.; Lhiaubet-Vallet, V.; Marin, M. L.; Miranda, M. A. *Chem. - Eur. J.* **2015**, *21*, 17051−17056.
(23) Mai, S.; Marquetand, P.; González, L. *Int. J. Quantum Chem.* **2015**, *115*, 1215−1231.
(24) Richter, M.; Marquetand, P.; González-Vázquez, J.; Sola, I.; González, L. *J. Chem. Theory Comput.* **2011**, *7*, 1253−1258.
(25) Knowles, P. J.; Werner, H. J. *Chem. Phys. Lett.* **1985**, *115*, 259−267.
(26) Hoffmann, R.; Woodward, R. B. *Acc. Chem. Res.* **1968**, *1*, 17−22.
(27) Bernardi, F.; Olivucci, M.; Robb, M. A. *Acc. Chem. Res.* **1990**, *23*, 405−412.
(28) Caldwell, R. A. *J. Am. Chem. Soc.* **1980**, *102*, 4004−4007.
(29) McCullagh, M.; Hariharan, M.; Lewis, F. D.; Markovitsi, D.; Douki, T.; Schatz, G. C. *J. Phys. Chem. B* **2010**, *114*, 5215−5221.
(30) Ando, H.; Fingerhut, B. P.; Dorfman, K. E.; Biggs, J. D.; Mukamel, S. *J. Am. Chem. Soc.* **2014**, *136*, 14801−14810.
(31) Barbatti, M. *ChemPhysChem* **2014**, *15*, 3342−3354.
(32) Zhang, W.; Yuan, S.; Li, A.; Dou, Y.; Zhao, J.; Fang, W. *J. Phys. Chem. C* **2010**, *114*, 5594−5601.
(33) Law, Y. K.; Azadi, J.; Crespo-Hernández, C. E.; Olmon, E.; Kohler, B. *Biophys. J.* **2008**, *94*, 3590−3600.
(34) Shui, X.; McFail-Isom, L.; Hu, G. G.; Williams, L. D. *Biochemistry* **1998**, *37*, 8341−8355.
(35) Smith, M. B.; Michl, J. *Chem. Rev.* **2010**, *110*, 6891−6936.
(36) Serrano-Pérez, J. J.; González-Luque, R.; Merchán, M.; Serrano-Andrés, L. *J. Phys. Chem. B* **2007**, *111*, 11880−11883.
(37) Melaccio, F.; Olivucci, M.; Lindh, R.; Ferré, N. *Int. J. Quantum Chem.* **2011**, *111*, 3339−3346.
(38) Wang, J.; Cieplak, P.; Kollman, P. A. *J. Comput. Chem.* **2000**, *21*, 1049−1074.
(39) Finley, J.; Malmqvist, P. A.; Roos, B. O.; Serrano-Andrés, L. *Chem. Phys. Lett.* **1998**, *288*, 299−306.
(40) Plasser, F.; Lischka, H. *J. Chem. Theory Comput.* **2012**, *8*, 2777−2789.
(41) Plasser, F.; Wormit, M.; Dreuw, A. *J. Chem. Phys.* **2014**, *141*, 024106.

DOI: 10.1021/jacs.6b06701
J. Am. Chem. Soc. 2016, 138, 15911−15916